Available online at www.sciencedirect.com
ScienceDirect
Journal of Power Sources 178 (2008) 118–124
JOURNAL OF POWER SOURCES
www.elsevier.com/locate/jpowsour

A small mono-polar direct methanol fuel cell stack with passive operation

Y.H. Chan, T.S. Zhao *, R. Chen, C. Xu

Department of Mechanical Engineering, The Hong Kong University of Science and Technology, Clear Water Bay, Kowloon, Hong Kong SAR, China

Received 2 November 2007; received in revised form 7 December 2007; accepted 10 December 2007
Available online 23 December 2007

Abstract

A passive direct methanol fuel cell (DMFC) stack that consists of six unit cells was designed, fabricated, and tested. The stack was tested with different methanol concentrations under ambient conditions. It was found that the stack performance increased when the methanol concentration inside the fuel tank was increased from 2.0 to 6.0 M. The improved performance is primarily due to the increased cell temperature as a result of the exothermic reaction between the permeated methanol and oxygen on the cathode. Moreover, the increased cell temperature enhanced the water evaporation rate on the air-breathing cathode, which significantly reduced water flooding on the cathode and further improved the stack performance. This passive DMFC stack, providing 350 mW at 1.8 V, was successfully applied to power a seagull display kit. The seagull display kit can continuously run for about 4 h on a single charge of 25 cm^3 4.0-M methanol solution.

Keywords: Passive DMFC; Stack; Methanol crossover; Temperature; Portable power source

1. Introduction

Recently, there has been considerable interest in the use of direct methanol fuel cells (DMFCs) as the replacement of conventional batteries for powering portable electronic devices, such as laptop computers, MP3 players, and cellular phones. The advantages offered by the DMFC include high energy density, low emission and ease in handling fuel. Therefore, extensive efforts have been exerted on the study of the DMFC, among which most of the researches focused on active DMFCs with fuel fed by liquid pumps and oxidant fed by gas compressors/blowers [1–8]. In portable applications, however, the parasitic energy losses caused by the ancillary devices in active DMFCs, such as methanol fuel supply devices, air blowers, heat exchangers, etc., become relatively large, which will significantly reduce the volumetric power density and the overall efficiency of the fuel cell system. To make the fuel cell system more compact and to reduce the parasitic energy losses associated with ancillary devices, the concept of passive DMFCs, in which both the fuel and oxidant are supplied passively have been proposed and investigated [9–21]. This type of fuel cell not only eliminates the parasitic power losses due to the ancillary devices required in conventional active DMFCs but also offers a simple and compact system. Because of these advantages, the passive DMFC has received much more attention in recent years.

Over the past decade, most of previous investigations concerning the passive DMFC were focused on single cells. However, to fulfill the requirement of a real application, a higher output of the passive DMFC system is required. Hence, the development of the passive DMFC stack is essential, in which single cells are connected in series or in parallel. Chang et al. [22] reported a DMFC stack with 12 cells connected in series. The active area for each cell in the stack was 2.0 cm^2. The DMFC stack can provide a peak power output of 560 mW at 2.8 V. Chen and Yang [15] developed an air-breathing DMFC stack that consisted of four cells. A maximum power output of 342 mW at 1 V was achieved.

Although a few papers have been reported on the air-breathing DMFC stack, the details of the stack design and fabrication are not addressed in the literature. Hence, the objective of this work is to design, fabricate and test a passive DMFC stack that operates at room temperature. Then we investigated the effect of methanol concentration on the performance of the passive DMFC stack. In addition, the effect of cell operating temperature on the water flooding at the air-breathing cathode

* Corresponding author. Tel.: +852 2358 8647; fax: +852 2358 1543.
E-mail address: metzhao@ust.hk (T.S. Zhao).

0378-7753/$ – see front matter © 2008 Elsevier B.V. All rights reserved.
doi:10.1016/j.jpowsour.2007.12.039

was also studied. Finally, the passive DMFC prototype was successfully applied to power a seagull display kit.

2. Experimental

2.1. Cell design

The overall design of the mono-polar stack is shown in Fig. 1. This stack consists of one middle plate with a built-in fuel tank, two mono-polar plates with three unit cells and two end plates. Details are described as follows.

2.1.1. Middle plate

The function of the middle plate is twofold: to store the fuel and to provide the support to each unit cell. In this work, transparent acrylic was used to fabricate the middle plate, which can provide not only a sufficient rigidity to support the unit cells, but also a rather low electrical conductivity to prevent short circuits between current collectors. Moreover, because of its low thermal conductivity, the heat loss from the stack can be reduced such that the cell operating temperature can be increased. Three pockets were machined on the middle plate and served as the built-in fuel tank with total volume of 25 mL, as shown in Fig. 1. These pockets were connected by the drilled ducts to ensure the uniform distribution of methanol concentration in the built-in fuel tank.

2.1.2. Mono-polar plates

Two mono-polar plates with three unit cells were fixed on the both sides of the middle plate with the anodic side facing to the fuel tank. For each mono-polar plate, three unit cells are placed side by side with the same polarity on the same side of the MEA and with their anodes and cathodes connected in series. The structure of the mono-polar plate is shown in Fig. 2, which consists of a fixer plate, three membrane electrode assemblies (MEAs) sandwiched by three anode and cathode current collectors. The unit cells were connected by bolts and nuts, as sketched in Fig. 3. The anode of each unit cell was connected to the cathode of the adjacent unit cell by bolts and nuts. The position of each unit cell was fixed by the machined pocket on the fixer plate. Additionally, gaskets made of silicon rubber were added between the mono-polar plates and the middle plate to prevent methanol leakage from the fuel tank. During the stack assembly process, these two mono-polar plates along with the middle plate and end plates were clamped by eight M4 screw joints, each having a torque of about 5 Nm.

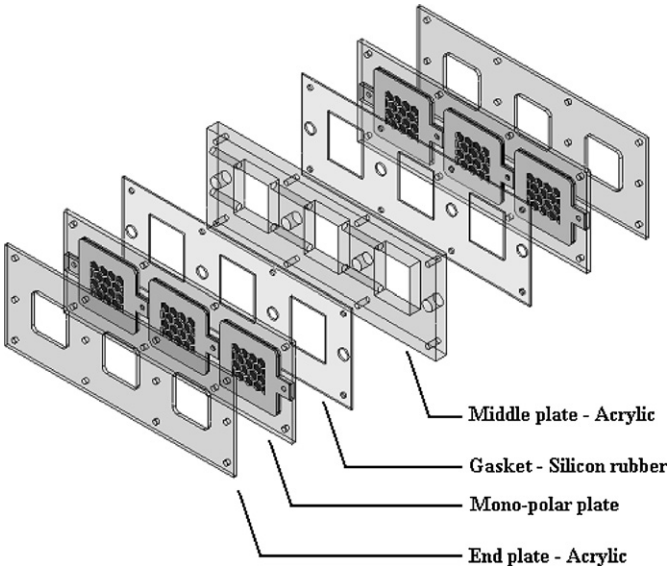

Fig. 1. Schematic of the passive DMFC stack.

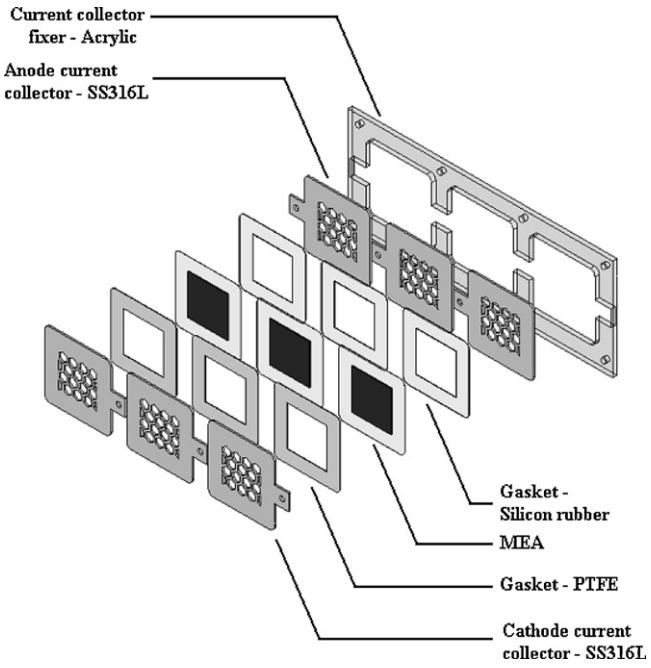

Fig. 2. Schematic of the mono-polar plate.

2.1.3. Current collector

The current collector is one of the key components of the unit cell, which serves not only for conducting the electricity but also for delivering the fuel and oxidant. Furthermore, because a large pressure is typically applied onto the current collectors to enhance the contact between the current collectors and electrodes so as to reduce the contact electrical resistance, it is essential to employ the material with high stiffness as the current collectors. As a consequence, the material used for the current collectors requires good electrical conductivity and high stiffness. In this work, 316L stainless steel plate with the thickness of 1.0 mm was used, which provides not only sufficient stiffness but also high electrical conductivity and corrosive resistance. A plurality of hexagonal holes were machined on both anode and cathode current collectors shown in Fig. 4, providing the passages of fuel and oxidant, which resulted in an open ratio of 53.6%. A 200-nm platinum layer was sputtered onto the surface of the current collectors to further reduce the contact resistance with the electrodes.

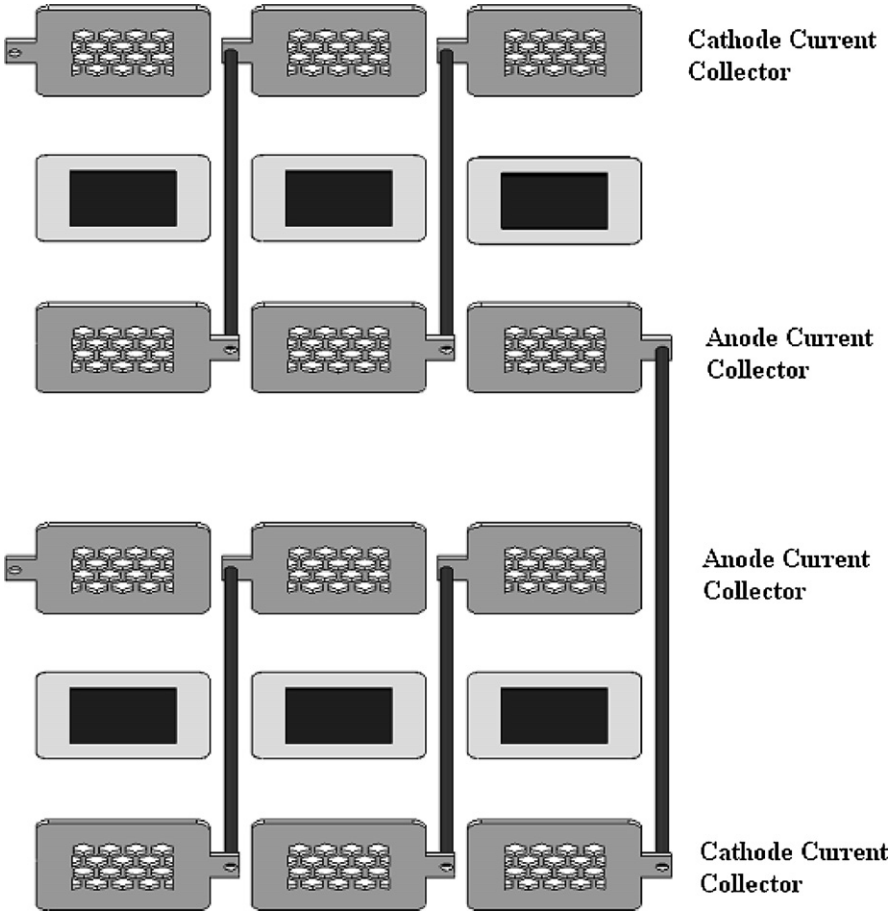

Fig. 3. Schematic of the connection of the unit cells by bolts and nuts.

2.1.4. Gasket

In order to prevent the leakage of methanol from the anode to cathode, gaskets were added between the current collectors and the edged membrane of each MEA. Since both the sealing and contact resistance largely depends on the material and thickness of the gasket, properly selecting the gasket is crucial in the stack design. For a given pressure, the use of a thinner gasket usually results in a larger gap between the current collector and gasket, which tends to increase the leakage of methanol solution. However, the use of too thick gaskets will cause a poor contact between an electrode and a current collector, which increases contact resistance. Hence, proper gaskets were selected to minimize the contact resistance between the current collectors and electrodes while preventing the methanol solution leakage. To this end, silicon rubber and PTFE sheets were selected on the anode and cathode, respectively. As shown in Fig. 5, the gasket made of silicon rubber was employed on the anode side of the MEA. The high compressibility of the silicon rubber provided good contact between the edged membrane and current collector, which resulted in a good sealing to prevent the leakage of methanol solution. The gasket made of PTFE was employed on the cathode side of the MEA. By selecting the proper thickness gasket made by PTFE, the compression of the silicon rubber can be controlled to achieve sufficient sealing and good contact between the electrodes and current collectors due to the relatively lower compressibility of PTFE. In this work, the 0.5 mm silicon rubber sheet and 0.25 mm PTFE sheet were chosen as the gaskets on the anode and cathode, respectively.

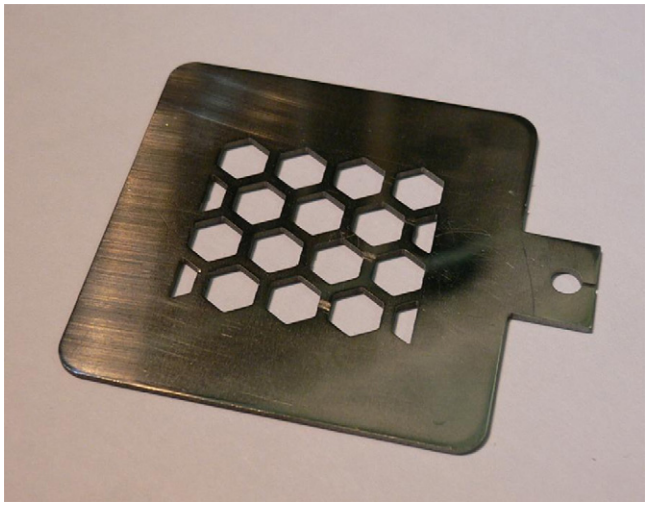

Fig. 4. Current collector with hexagonal holes.

2.1.5. Membrane electrode assembly

Six membrane electrode assemblies (MEAs), each with an active area of 6.25 cm^2, were fabricated with single-side ELAT

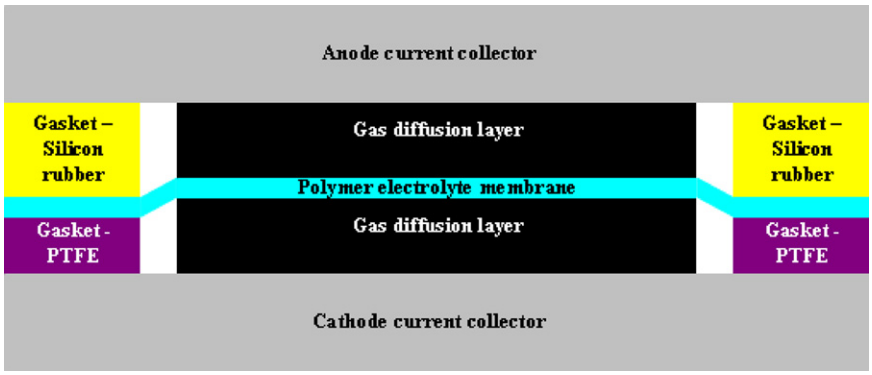

Fig. 5. Configuration of the MEA with gasket.

electrodes from ETEK in both the anode and the cathode. Both electrodes use carbon cloth (E-TEK, Type A) with 30 wt.% PTFE wet-proofing treatment as the backing support layer. The catalyst loading on the anode side is 4.0 mg cm^{-2} with PtRu black (1:1, a/o), while the catalyst loading on the cathode side is 2.0 mg cm^{-2} using 40 wt.% Pt on Vulcan XC-72. Furthermore, 0.8 mg cm^{-2} dry Nafion ionomer was coated onto the surface of each electrode. Pretreated Nafion 115 membrane was employed as the electrolyte. The pretreatment process included boiling the membrane in 5 vol% H_2O_2, washing in DI water, boiling in 0.5 M H_2SO_4 and washing in DI water for 1 h in each turn. Finally, MEAs with active area of 6.25 cm^2 were fabricated by hot pressing at 135 °C at 2 MPa for 20 min. More detailed information about the MEA fabrication can be found elsewhere [23].

2.2. Electrochemical instrumentation and testing condition

An Arbin BT2000 electrical load interfaced to a computer was employed to control the condition of discharging and record the voltage–current curves. All the experiments of the passive DMFC stack were performed at room temperature of 21–23 °C and relative humidity of 75–81%.

3. Results and discussion

3.1. Stack performance with different methanol concentrations

Fig. 6 shows the performance of the passive DMFC stack that operated with various methanol concentrations from 2.0 to 6.0 M. It is seen that the performance of the stack increased with an increase in methanol concentration, including the limiting current density and the peak power density. It is also seen that the increment of performance was relatively small when methanol concentration was increased from 2.0 to 3.0 M. As methanol concentration was increased from 3.0 to 4.0 M, the peak power density exhibited a much larger increment. However, when methanol concentration was further increased to 6.0 M, the increment became smaller, which was similar to the difference between 2.0 and 3.0 M. A maximum power density of 10.3 mW cm^{-2} was obtained with 6.0 M methanol operation. The detailed performance parameters are listed in Table 1. It is seen from Table 1 that the maximum power density increased from 5.8 to 10.3 mW cm^{-2} as methanol concentration increased from 2.0 to 6.0 M. However, the open-circuit voltage (OCV) decreased with increasing methanol concentration. This can be attributed to the fact that the rate of methanol crossover increases with the methanol concentration. The increased rate of methanol crossover caused a larger mixed potential on the cathode, lowering the OCV and the cell voltage at low current densities. At high current densities, however, the performance increased with the methanol concentration. The reason leading to this phenomenon is described as follows. Firstly, the permeated methanol is electrochemically oxidized on the cathode to produce heat, causing an increase in the cell temperature. A higher rate of methanol crossover at the higher methanol concentration leads to a higher heat generation rate and thereby a higher cell operating temperature, as evidenced from the measured cell temperature shown in Fig. 7. The increased cell temperature enhances the electrochemical kinetics of methanol oxidation and oxygen reduction reactions. Therefore, higher methanol concentration yielded higher cell performance as a result of the enhanced electrochemical kinetics on both the anode and cathode resulting from the higher cell operating temperature.

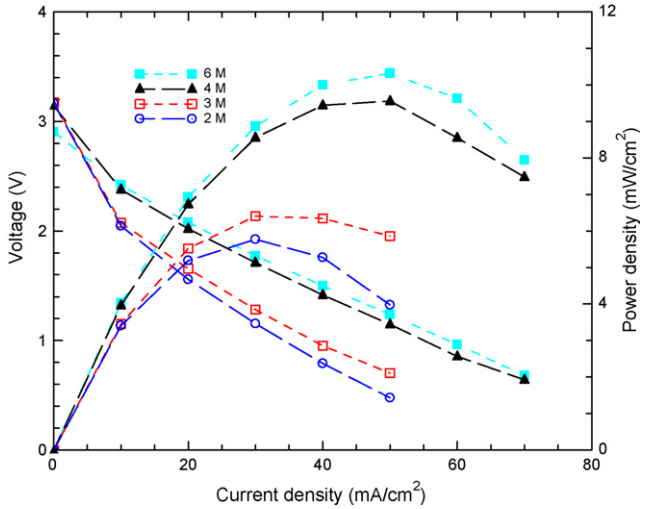

Fig. 6. Effect of methanol concentration on the performance of passive DMFC stack.

Table 1
The performance of the passive DMFC stack using different methanol concentrations

Methanol concentration (M)	Open circuit voltage (V)	Maximum power density (mW cm^{-2})	Maximum temperature (°C)
2.0	3.155	5.8	35.4
3.0	3.147	6.4	41.0
4.0	3.141	9.5	51.3
6.0	2.905	10.3	72.9

However, it should be noted that when the methanol concentration is further increased to 6.0 M, the adverse effect of methanol crossover becomes more significant. Although the cell operating temperature is further increased with higher methanol concentration operation, the improved performance as a result of the increased temperature is compensated by the increased mixed potential, leading to the smaller increment at 6.0 M operation. This fact indicates that the thermal management is crucial for the passive DMFC stack, which can be obtained by optimizing the stack design instead of increasing the methanol concentration. Secondly, the increased cell temperature can also reduce the water flooding on the air-breathing cathode as a result of the increased water evaporation rate, which enhances the oxygen transport and further improves the cell performance and operation stability. To demonstrate the effect of cell temperature on the water removal in the passive DMFC stack, we discharged a single cell and the stack at a constant current density of 50 mA cm^{-2} with methanol concentration of 4.0 M for 1.0 h, respectively, such that water generation rate in both the single cell and each unit cell of the stack are almost the same. However, the heat loss from the stack is much smaller than that in the single cell. This is because the heat is mainly lost from the cathode in the stack only, but the heat is lost from both the anode and cathode for the single cell. As a result, the stack exhibited a higher cell temperature than did the single cell. Moreover, the increased cell temperature increased the rate of methanol crossover, leading to a higher heat generation rate, which further increases the cell temperature of the stack. During the testing, it was found that the cell operating temperature of the stack (50–53 °C) was much higher than that of the single cell (27–29 °C). The increased cell operating temperature increases the water evaporation rate, reducing the water flooding on the air-breathing cathode. This can be evidenced by the captured liquid water behavior on the air-breathing cathode shown in Fig. 8. It can be seen from Fig. 8 that a large amount of water was accumulated on the cathode of the single cell while no liquid water was observed on the cathode of the stack as a result

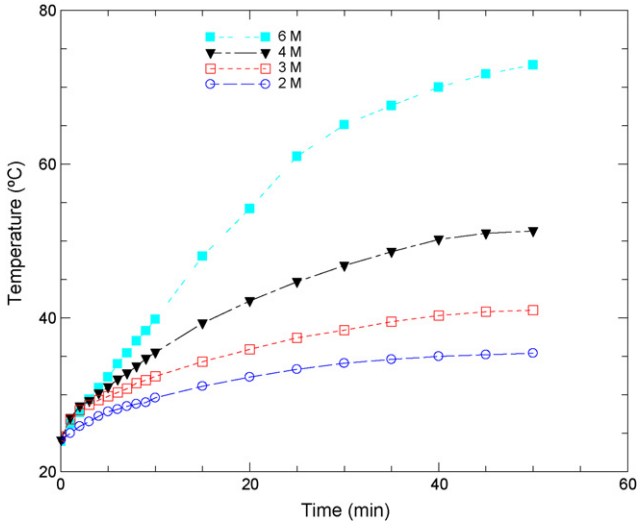

Fig. 7. Variation in stack temperature with different methanol concentrations.

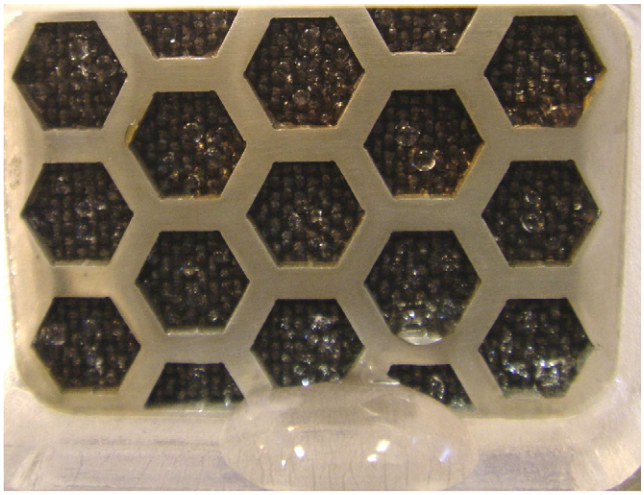

(a) Single cell

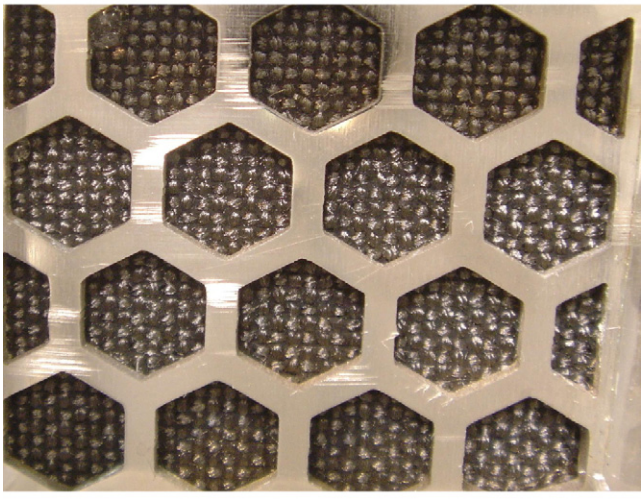

(b) Unit cell of the stack

Fig. 8. Water accumulation on the air-breathing cathode after 1.0 h operation with constant current density (50 mA cm^{-2}). (a) Single cell and (b) unit cell of the stack.

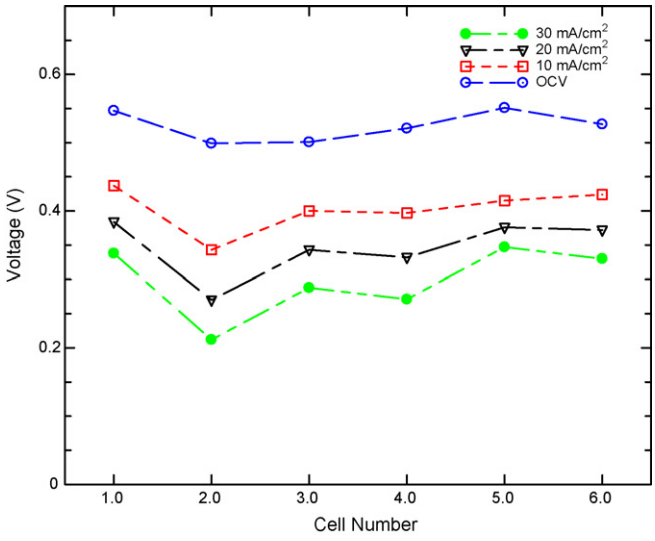

Fig. 9. Voltage of each unit cell in the stack at different current densities.

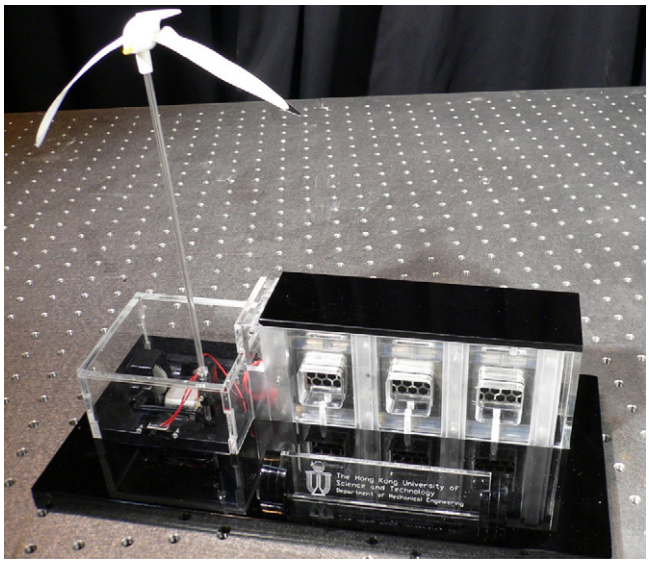

Fig. 10. Seagull display kit powered by passive DMFC stack.

of the increased water evaporation rate resulting from the higher cell operating temperature. Hence, although the water generation rates for both the single cell and unit cell of the stack are the same, water flooding on the air-breathing cathodes of the stack was minimized due to the higher water evaporation rate, leading to the improved cell performance. This fact also indicates that the thermal and water management are inherently coupled in the passive DMFC. The water management of the passive DMFC can be achieved by the optimal thermal management.

Fig. 9 shows the voltage profiles of the stack at different discharging current densities with 6.0 M methanol operation. For convenience of description, each single cell is designated with Arabic numerals from 1 to 6. It is seen that the distribution of the OCV in the stack is quite uniform, indicating that each unit cell was capable of yielding the same performance. However, with current density increasing, the variation in the cell voltage became larger. Particularly, Cell 2 yielded much lower performance than did the other cells at the load of 30 mA cm^{-2}. The lowered performance of Cell 2 was mainly due to the increased contact resistance between the current collectors and electrodes, which was caused by the non-uniformity of the applied pressure during the stack assembly. It was found that the internal resistance of Cell 2 (0.658 Ω) was much higher than those of other unit cells (0.207–0.551 Ω). Therefore, the stack assembly is critical for improving the uniformity of the passive DMFC stack.

3.2. Application of the passive DMFC stack to a seagull display kit

After finishing the stack performance test, this passive DMFC stack was applied to the seagull display kit to demonstrate their feasibility as portable power sources. The seagull display kit powered by the passive DMFC stack is shown in Fig. 10. The power required to operate the seagull is about 350 mW at 1.8 V. It was found that the seagull display kit could continuously operate for about 4 h with 25 mL of 4.0 M methanol solution.

4. Concluding remarks

A passive DMFC stack with six unit cells was designed, fabricated and tested. A maximum power density of 10.3 mW cm^{-2} was achieved with 6.0 M methanol operation under ambient temperature and passive conditions. It was found that the power density increased continuously when the fed methanol concentration was increased from 2.0 to 6.0 M. The improved performance of the passive DMFC stack working with higher methanol concentrations was mainly attributed to the higher cell temperature caused by the exothermic reaction between the permeated methanol and oxygen on the cathode. The increased cell operating temperature led to the enhanced electrochemical kinetics of methanol oxidation and oxygen reduction reactions and thereby the improved performance. Moreover, the increased cell operating temperature resulted in a higher water evaporation rate, reducing the water flooding on the air-breathing cathode. As a result, the cell performance and operation stability can be further improved. In addition, it was also found that assembling the stack is critical for improving the uniformity of passive DMFC stacks. Finally, to demonstrate that the passive DMFC could be used as a power source for small portable electronic devices, this passive DMFC stack was applied to power a seagull display kit, providing 350 mW at 1.8 V with 4.0 M methanol solution. The seagull display kit can continuously run for about 4 h on a single charge of 25 mL 4.0 M methanol solution.

Acknowledgement

The work described in this paper was fully supported by a grant from the Research Grants Council of the Hong Kong Special Administrative Region, China (Project No. 622706).

References

[1] C.K. Dyer, J. Power Sources 106 (2002) 31.

[2] Q. Ye, T.S. Zhao, H. Yang, et al., Electrochem. Solid-State Lett. 8 (2005) A52.
[3] X. Ren, T.E. Springer, T.A. Zawodzinski, et al., J. Electrochem. Soc. 147 (2000) 466.
[4] J. Prabhuram, T.S. Zhao, C.W. Wong, J.W. Guo, J. Power Sources 134 (2004) 1.
[5] Z. Qi, A. Kaufman, J. Power Sources 110 (2002) 177.
[6] A. Kuver, W. Vielstich, J. Power Sources (1998) 211.
[7] B. Guraua, E.S. Smotkin, J. Power Sources 112 (2002) 339.
[8] R. Jiang, D. Chu, J. Electrochem. Soc. 151 (2004) A69.
[9] J.J. Martin, W.M. Qian, H.J. Wang, et al., J. Power Sources 164 (2007) 287.
[10] T. Shimizu, T. Momma, M. Mohamedi, et al., J. Power Sources 137 (2004) 277.
[11] B.K. Kho, B. Bae, M.A. Scibioh, et al., J. Power Sources 142 (2005) 50.
[12] R. Chen, T.S. Zhao, Electrochem. Commun. 9 (2007) 718.
[13] J.G. Liu, T.S. Zhao, Z.X. Liang, et al., J. Power Sources 153 (2006) 61.
[14] R. Chen, T.S. Zhao, J. Power Sources 157 (2006) 351.
[15] C.Y. Chen, P. Yang, J. Power Sources 123 (2003) 37.
[16] J. Han, E.S. Park, J. Power Sources 112 (2002) 477.
[17] H.K. Kim, J.M. Oh, J.H. Kim, et al., J. Power Sources 162 (2006) 497.
[18] Y.J. Kim, B. Bae, M.A. Scibioh, et al., J. Power Sources 157 (2006) 253.
[19] R. Chen, T.S. Zhao, Electrochim. Acta 52 (2007) 4317.
[20] J.G. Liu, T.S. Zhao, R. Chen, et al., Electrochem. Commun. 7 (2005) 288.
[21] R. Chen, T.S. Zhao, J. Power Sources 152 (2005) 122.
[22] H. Chang, J.R. Kim, J.H. Cho, H.K. Kim, K.H. Choi, Solid State Ionics 148 (2002) 601.
[23] H. Yang, T.S. Zhao, Q. Ye, Electrochem. Commun. 6 (2004) 1098.